

Supporting Information

Enzymatic modification of dihydromyricetin by glucosylation and acylation, and its effect on the solubility and antioxidant activity

*David Rodriguez-Garcia,^a Jose L. Gonzalez-Alfonso,^a Carlos Uceda,^a Laura Barahona,^b Marta Ruiz-Nuñez,^c Antonio O. Ballesteros,^a Tom Desmet,^d Julia Sanz-Aparicio,^c Maria Fernandez-Lobato,^b and Francisco J. Plou,^{*a}*

^a Instituto de Catálisis y Petroleoquímica, CSIC, 28049 Madrid, Spain.

^b Centro de Biología Molecular Severo Ochoa, Universidad Autónoma de Madrid, 28049, Madrid, Spain.

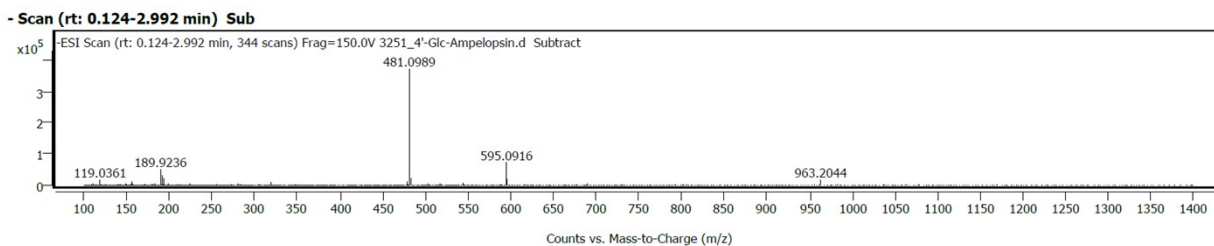
^c Instituto de Química Física Blas Cabrera, CSIC, 28006 Madrid, Spain.

^d Centre for Synthetic Biology (CSB), Department of Biotechnology, Ghent University, 9000 Ghent, Belgium.

INDEX

Figure S1	ESI-MS of dihydromyricetin 4'-O- α -D-glucopyranoside (1a) and 3'-O- α -D-glucopyranoside (1b)
Figure S2	^1H -NMR of dihydromyricetin 4'-O- α -D-glucopyranoside (1a)
Figure S3	^{13}C -NMR of dihydromyricetin 4'-O- α -D-glucopyranoside (1a)
Figure S4	2D-HMBC of dihydromyricetin 4'-O- α -D-glucopyranoside (1a)
Figure S5	^1H -NMR of dihydromyricetin 3'-O- α -D-glucopyranoside (1b)
Figure S6	^{13}C -NMR of dihydromyricetin 3'-O- α -D-glucopyranoside (1b)
Figure S7	2D-HMBC of dihydromyricetin 3'-O- α -D-glucopyranoside (1b)
Figure S8	
Figure S9	ESI-MS of dihydromyricetin 4'-O-(6-O-octanoyl)- α -D-glucopyranoside (2a), 4'-O-(6-O-lauroyl)- α -D-glucopyranoside (2b) and 4'-O-(6-O-palmitoyl)- α -D-glucopyranoside (2c)
Figure S10	^1H -NMR of dihydromyricetin 4'-O-(6-O-octanoyl)- α -D-glucopyranoside (2a)
Figure S11	^{13}C -NMR of dihydromyricetin 4'-O-(6-O-octanoyl)- α -D-glucopyranoside (2a)
Figure S12	2D-HMBC of dihydromyricetin 4'-O-(6-O-octanoyl)- α -D-glucopyranoside (2a)
Figure S13	^1H -NMR of dihydromyricetin 4'-O-(6-O-lauroyl)- α -D-glucopyranoside (2b)
Figure S14	^{13}C -NMR of dihydromyricetin 4'-O-(6-O-lauroyl)- α -D-glucopyranoside (2b)
Figure S15	2D-HMBC of dihydromyricetin 4'-O-(6-O-lauroyl)- α -D-glucopyranoside (2b)
Figure S16	^1H -NMR of dihydromyricetin 4'-O-(6-O-palmitoyl)- α -D-glucopyranoside (2c)
Figure S17	^{13}C -NMR of dihydromyricetin 4'-O-(6-O-palmitoyl)- α -D-glucopyranoside (2c)
Figure S18	2D-HMBC of dihydromyricetin 4'-O-(6-O-palmitoyl)- α -D-glucopyranoside (2c)

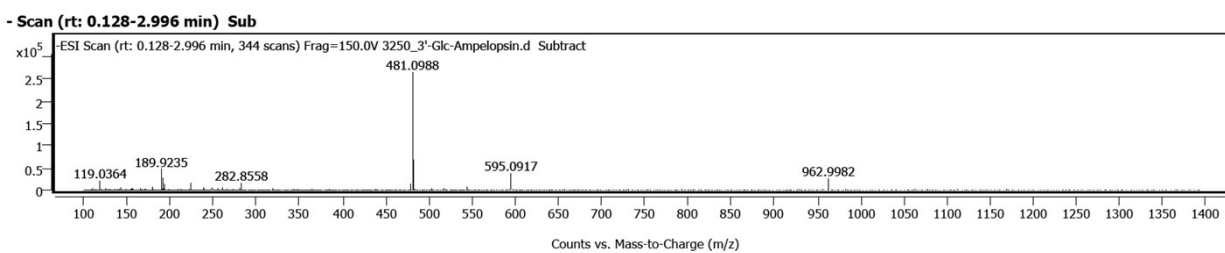
1a



Spectrum Peaks

m/z	Z	Abund	Abund %
119.0361		17137	4.63
189.9236		50273	13.57
191.9206		31640	8.54
193.9193		21601	5.83
481.0989	1	370473	100.00
482.1021	1	91145	24.60
483.1039	1	22137	5.98
595.0916	1	72713	19.63
596.0946	1	20246	5.47
963.2044		16869	4.55

1b



Spectrum Peaks

m/z	Z	Abund	Abund %
119.0364		20633	7.78
189.9235		46927	17.69
191.9204		27709	10.45
223.9276		14826	5.59
282.8558		15870	5.98
481.0988	1	265225	100.00
482.1020	1	67242	25.35
483.1039	1	15724	5.93
595.0917		37518	14.15
962.9982		26200	9.88

Figure S1. ESI-MS of dihydromyricetin 4'-O- α -D-glucopyranoside (**1a**) and dihydromyricetin 3'-O- α -D-glucopyranoside (**1b**)

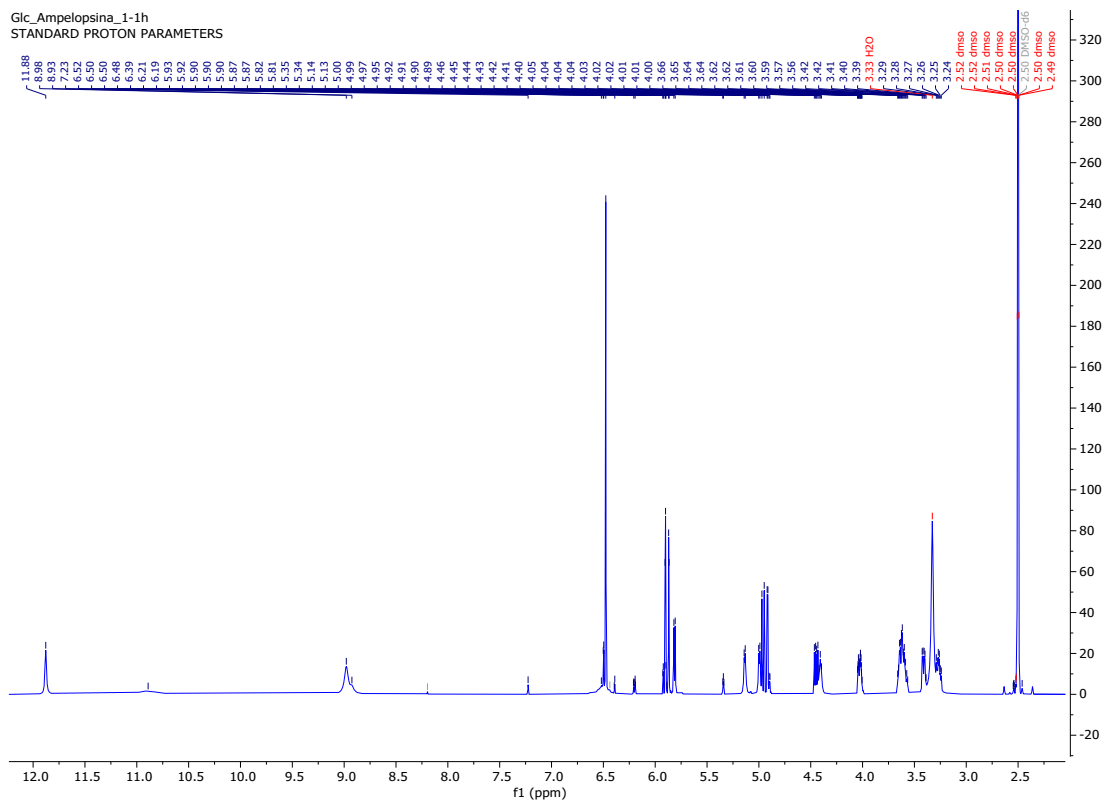


Figure S2. ^1H -NMR of dihydromyricetin 4'-O- α -D-glucopyranoside (**1a**)

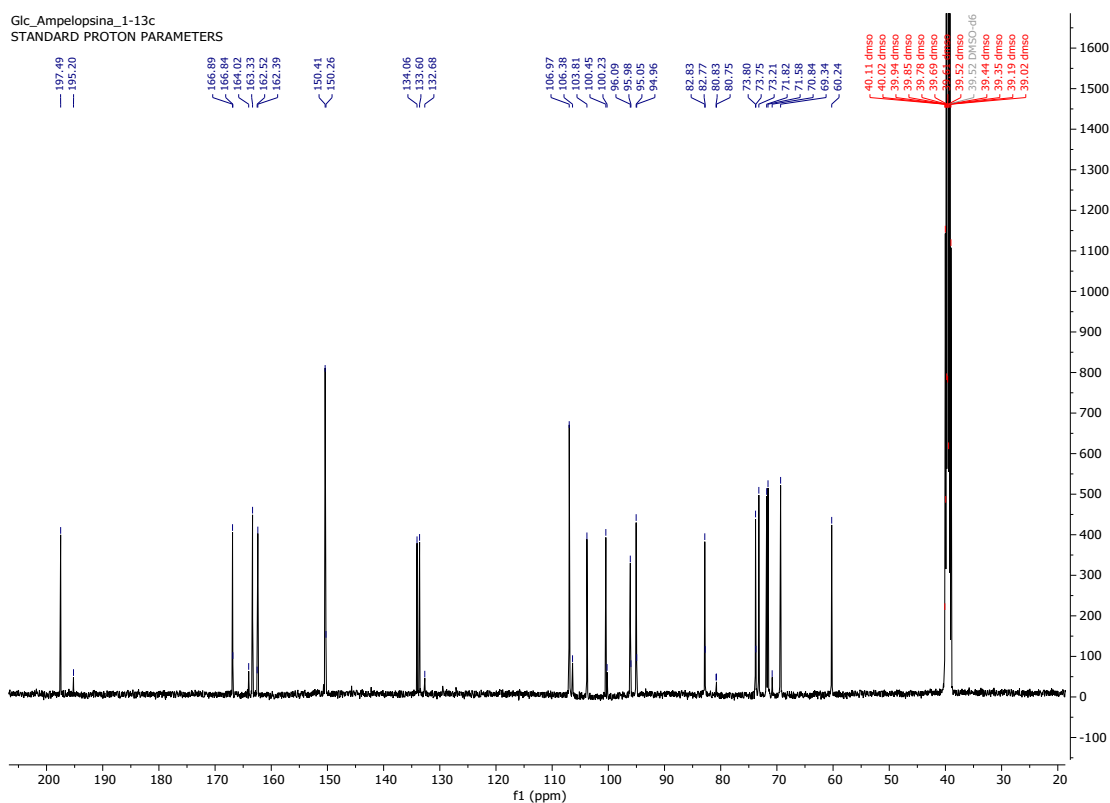


Figure S3. ^{13}C -NMR of dihydromyricetin 4'-O- α -D-glucopyranoside (**1a**)

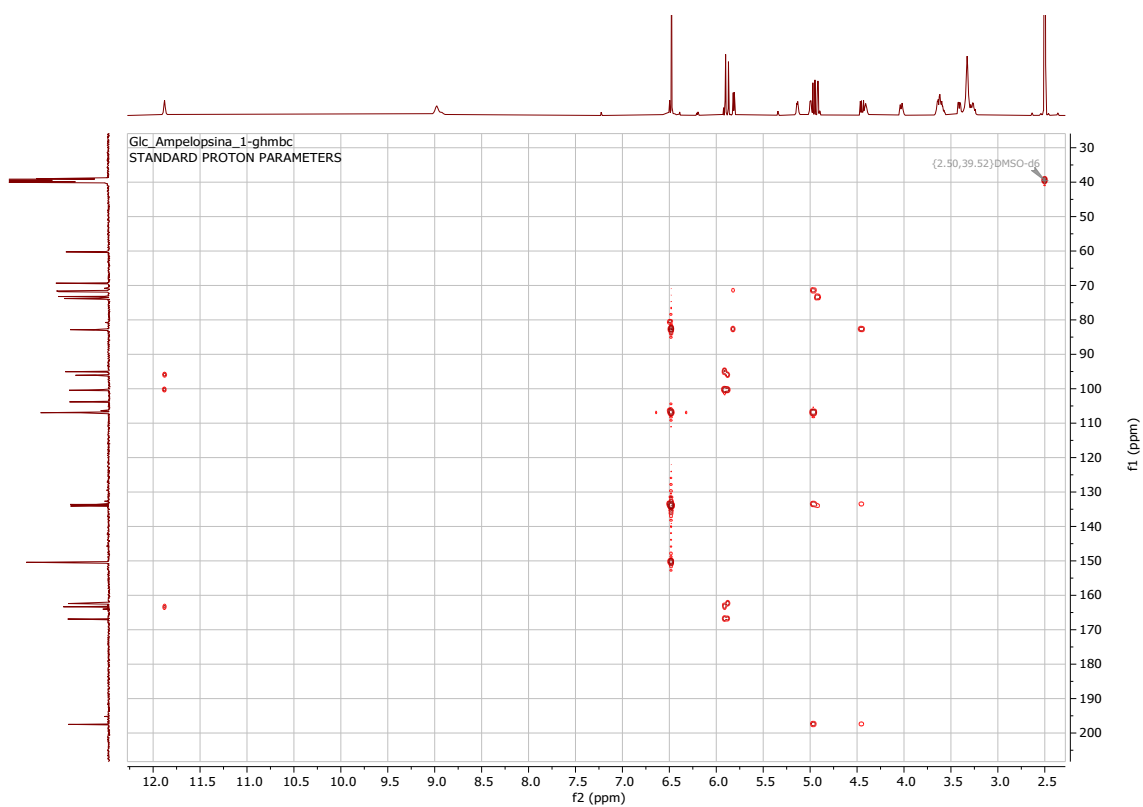


Figure S4. 2D-HMBC of dihydromyricetin 4'-O- α -D-glucopyranoside (**1a**)

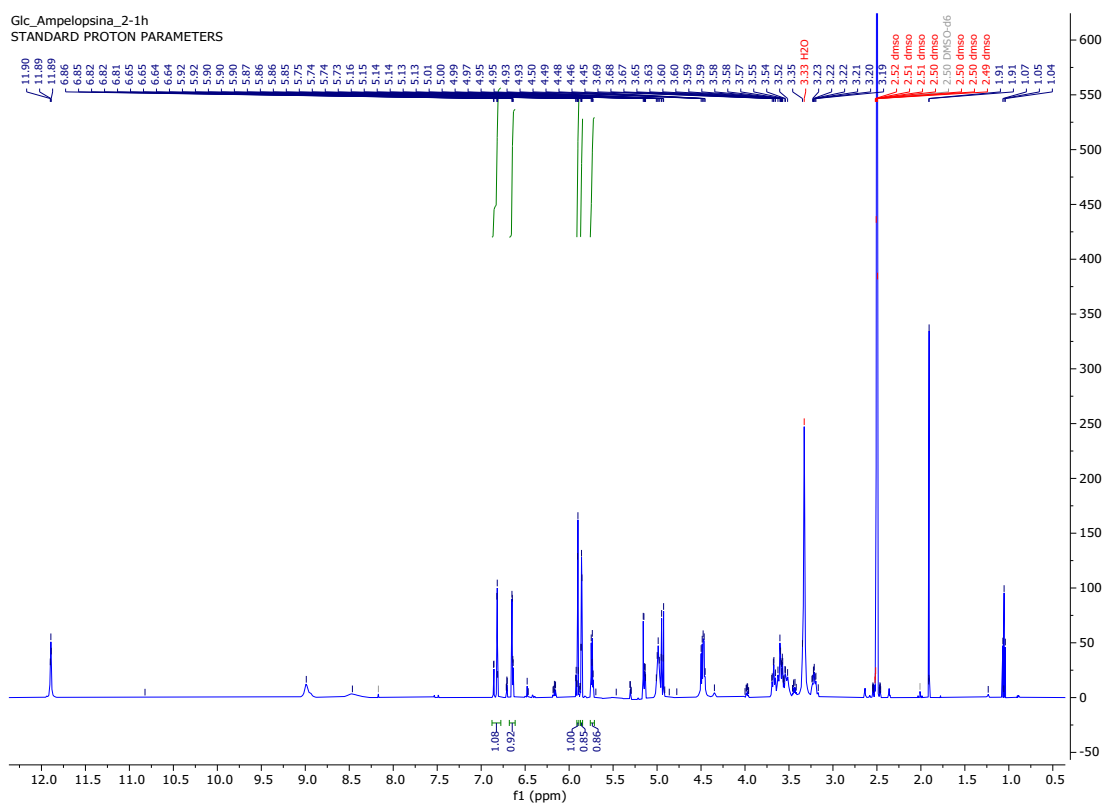


Figure S5. $^1\text{H-NMR}$ of dihydromyricetin 3'-O- α -D-glucopyranoside (**1b**)

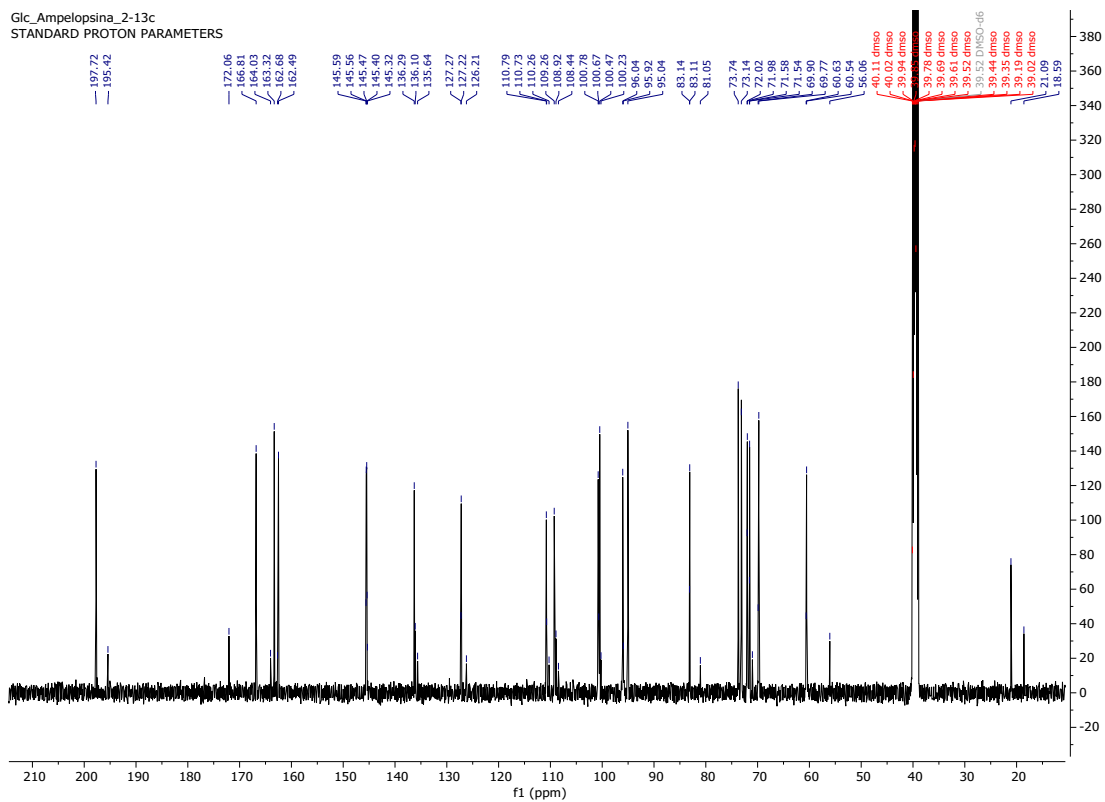


Figure S6. ^{13}C -NMR of dihydromyricetin 3'-O- α -D-glucopyranoside (**1b**)

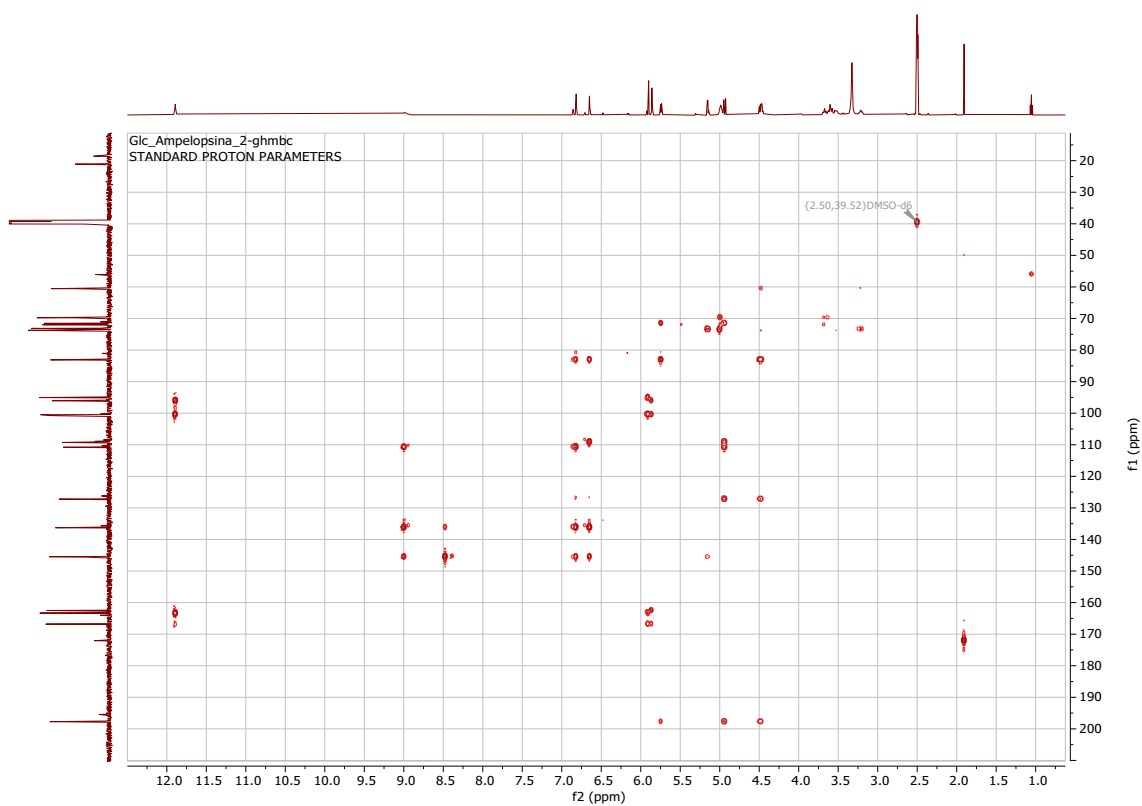


Figure S7. 2D-HMBC of dihydromyricetin 3'-O- α -D-glucopyranoside (**1b**).

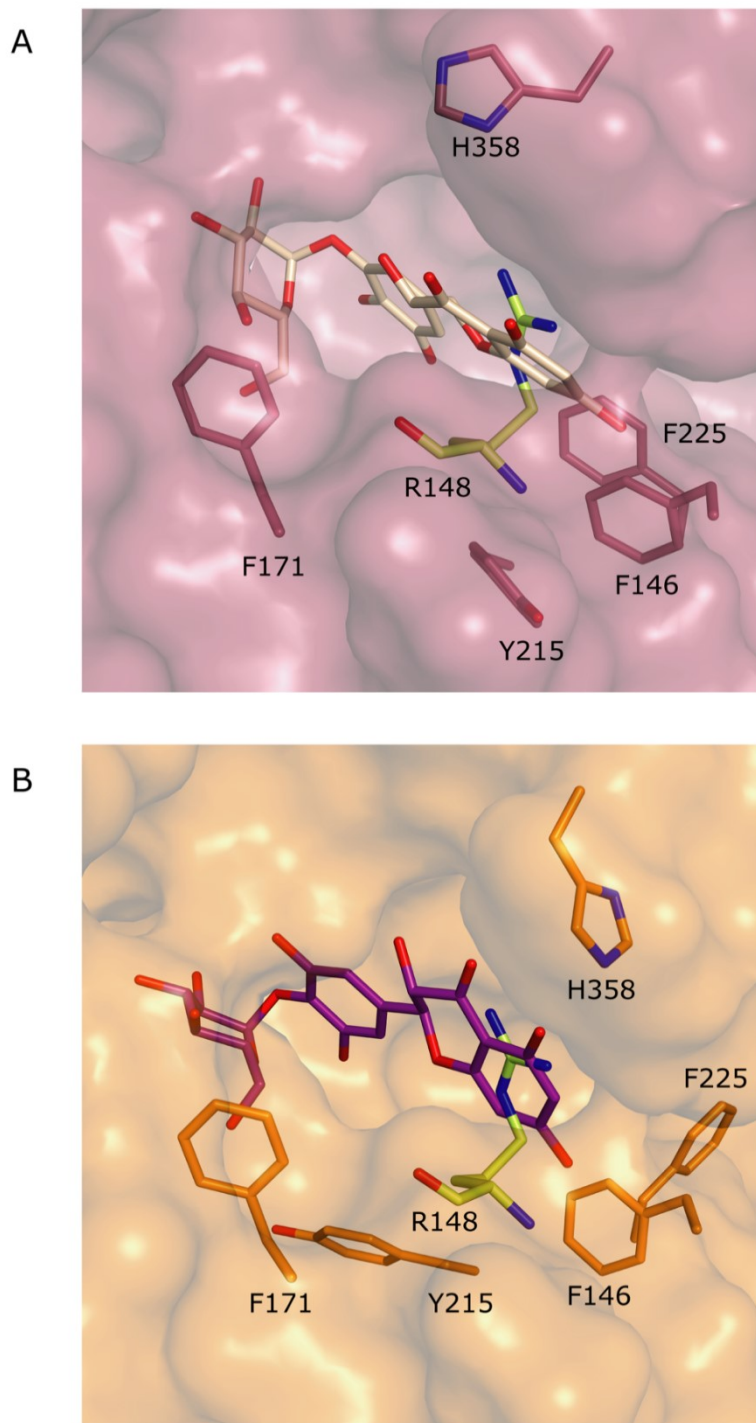
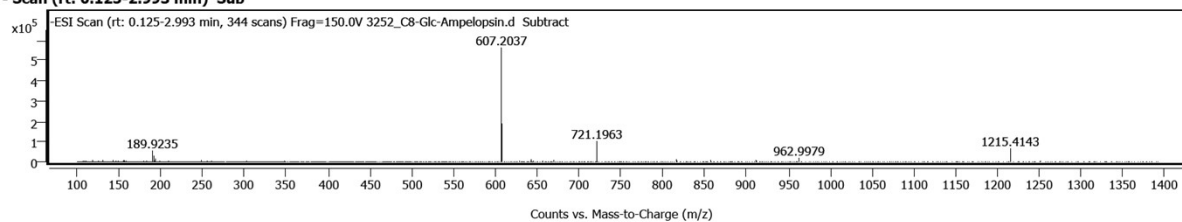


Figure S8. Impact of the R134A change (referred to as A148 in the text) on the binding pocket in the fitted structure. Docking simulation of the **(A)** 3'-O- α -D-glucopyranoside and **(B)** 4'-O- α -D-glucopyranoside into the TtSPP_R134A variant, represented as molecular surface. The final docked conformations of the flexible residues are shown as sticks. The position of Arg148 in the superimposed native enzyme is highlighted in green sticks.

Sample Spectra

- Scan (rt: 0.125-2.993 min) Sub

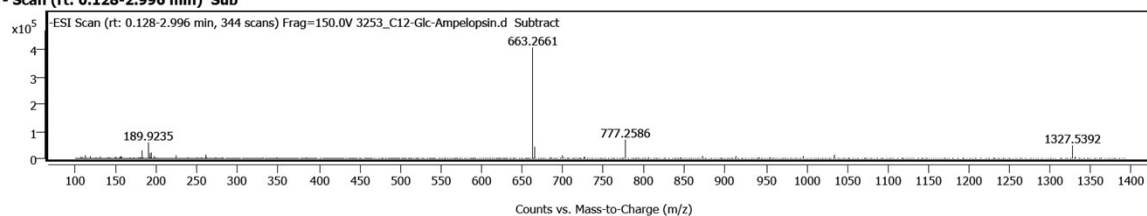


Spectrum Peaks

m/z	Z	Abund	Abund %
189.9235		53361	9.48
191.9205		31222	5.55
607.2037	1	563064	100.00
608.2065	1	186366	33.10
609.2087	1	49142	8.73
721.1963	1	101063	17.95
722.1994	1	36146	6.42
962.9979		19654	3.49
1215.4143	1	66027	11.73
1216.4174	1	44243	7.86

Sample Spectra

- Scan (rt: 0.128-2.996 min) Sub

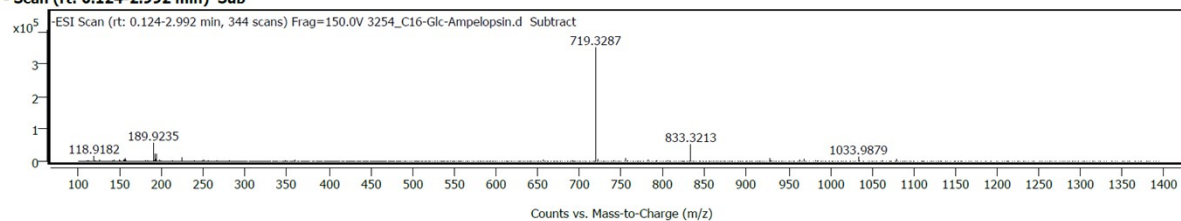


Spectrum Peaks

m/z	Z	Abund	Abund %
181.9292		29113	7.13
189.9235		56695	13.89
193.9192		20371	4.99
663.2661	1	408264	100.00
664.2691	1	153778	37.67
665.2713	1	42176	10.33
777.2586	1	68374	16.75
778.2620	1	28133	6.89
1327.5392	1	46635	11.42
1328.5422	1	36415	8.92

Sample Spectra

- Scan (rt: 0.124-2.992 min) Sub



Spectrum Peaks

m/z	Z	Abund	Abund %
118.9182		17340	4.90
189.9235		57693	16.30
191.9205		22277	6.29
193.9192		22609	6.39
719.3287	1	353945	100.00
720.3318	1	149897	42.35
721.3340	1	42807	12.09
833.3213	1	53068	14.99
834.3244	1	23939	6.76
1033.9879		13942	3.94

Figure S9. ESI-MS of dihydromyricetin 4'-O-(6-O-octanoyl)- α -D-glucopyranoside (**2a**), 4'-O-(6-O-lauroyl)- α -D-glucopyranoside (**2b**) and 4'-O-(6-O-palmitoyl)- α -D-glucopyranoside (**2c**).

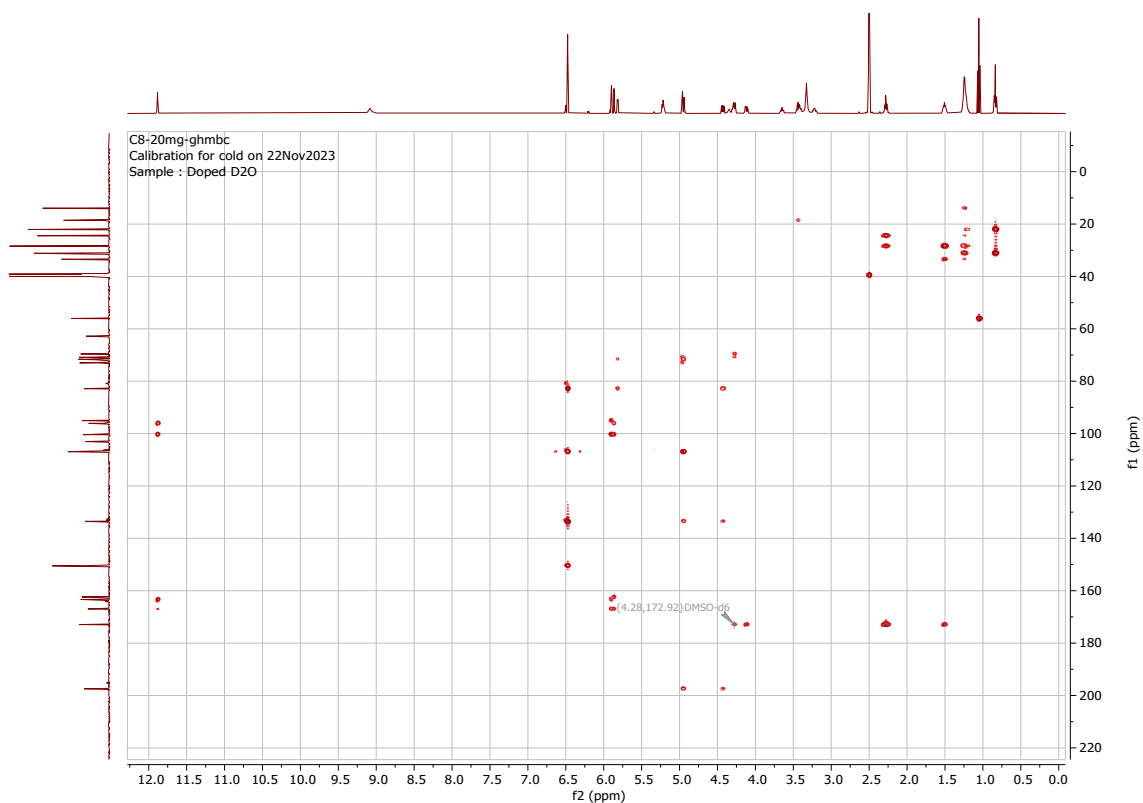


Figure S12. 2D-HMBC of dihydromyricetin 4'-O-(6-O-octanoyl)- α -D-glucopyranoside (**2a**)

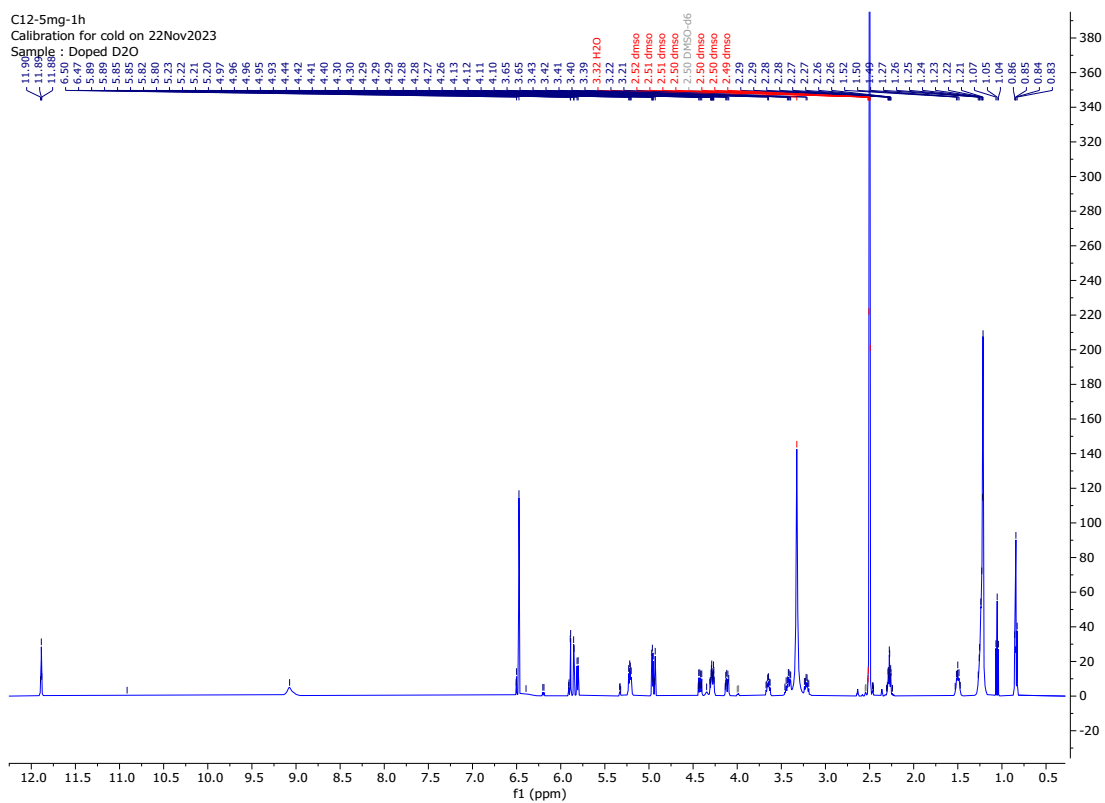


Figure S13. ^1H -NMR of dihydromyricetin 4'-O-(6-O-lauroyl)- α -D-glucopyranoside (**2b**)

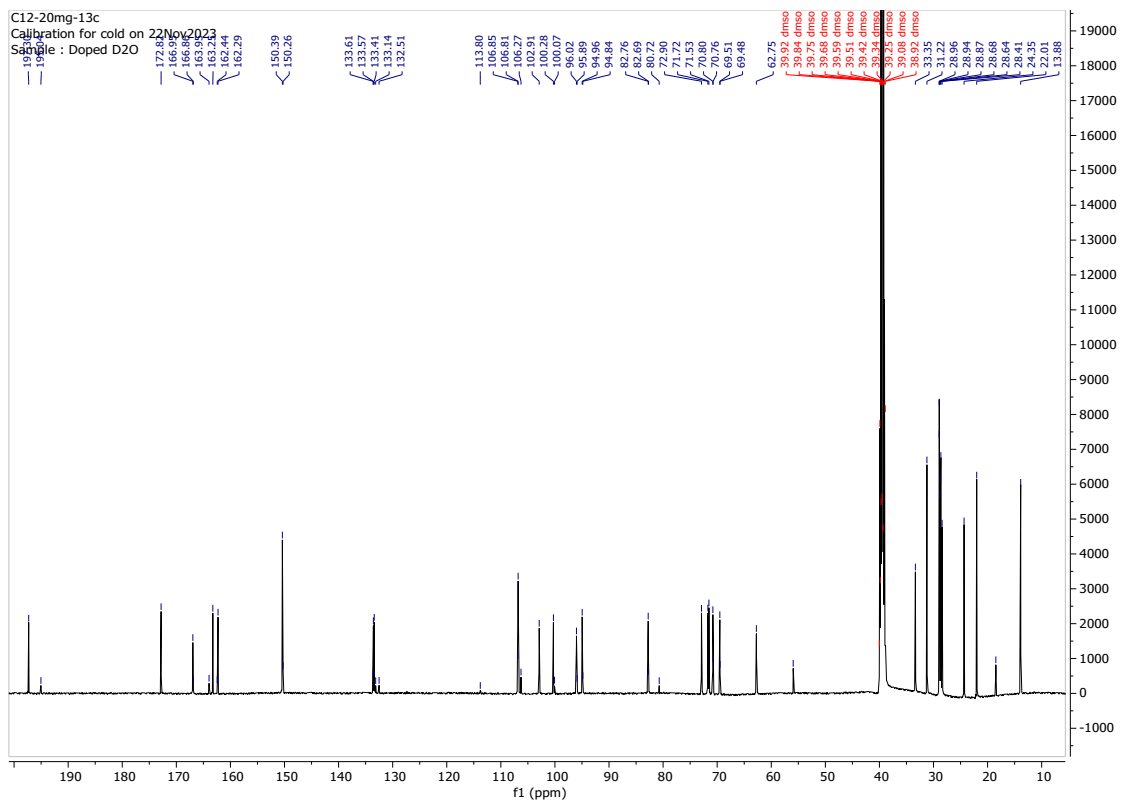


Figure S14. ^{13}C -NMR of dihydromyricetin 4'-O-(6-O-lauroyl)- α -D-glucopyranoside (**2b**)

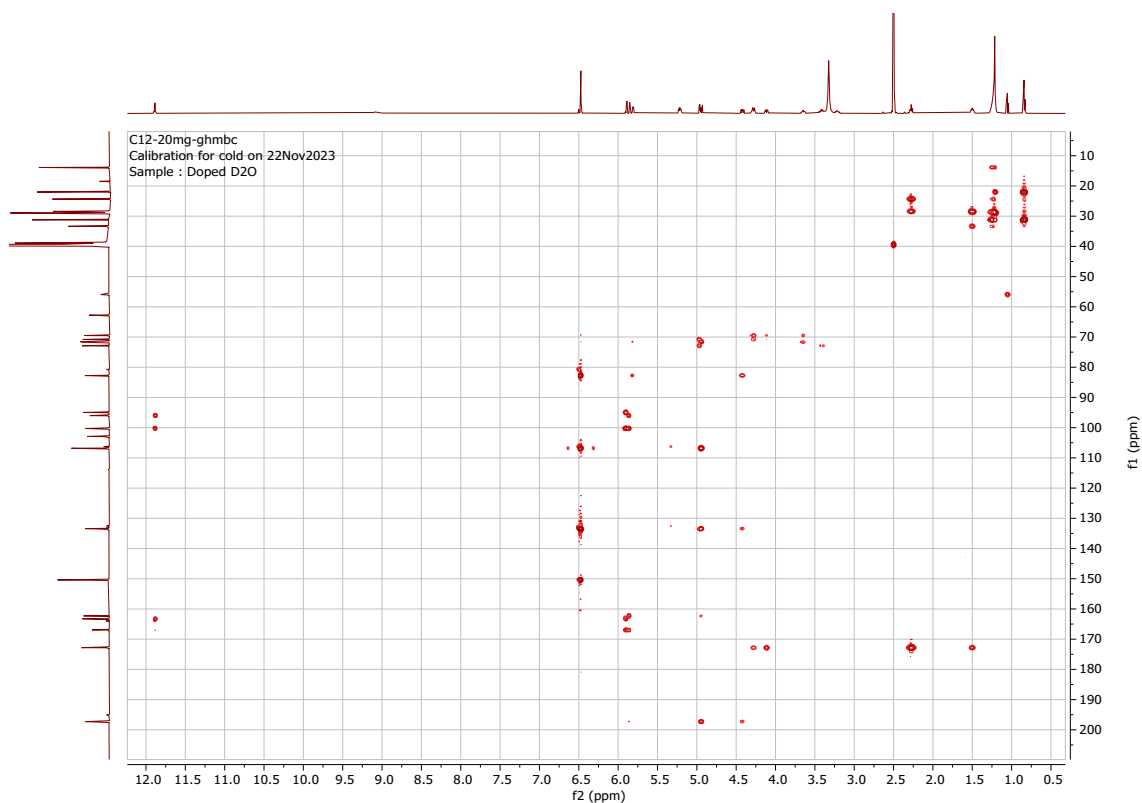


Figure S15. 2D-HMBC of dihydromyricetin 4'-O-(6-O-lauroyl)- α -D-glucopyranoside (**2b**)

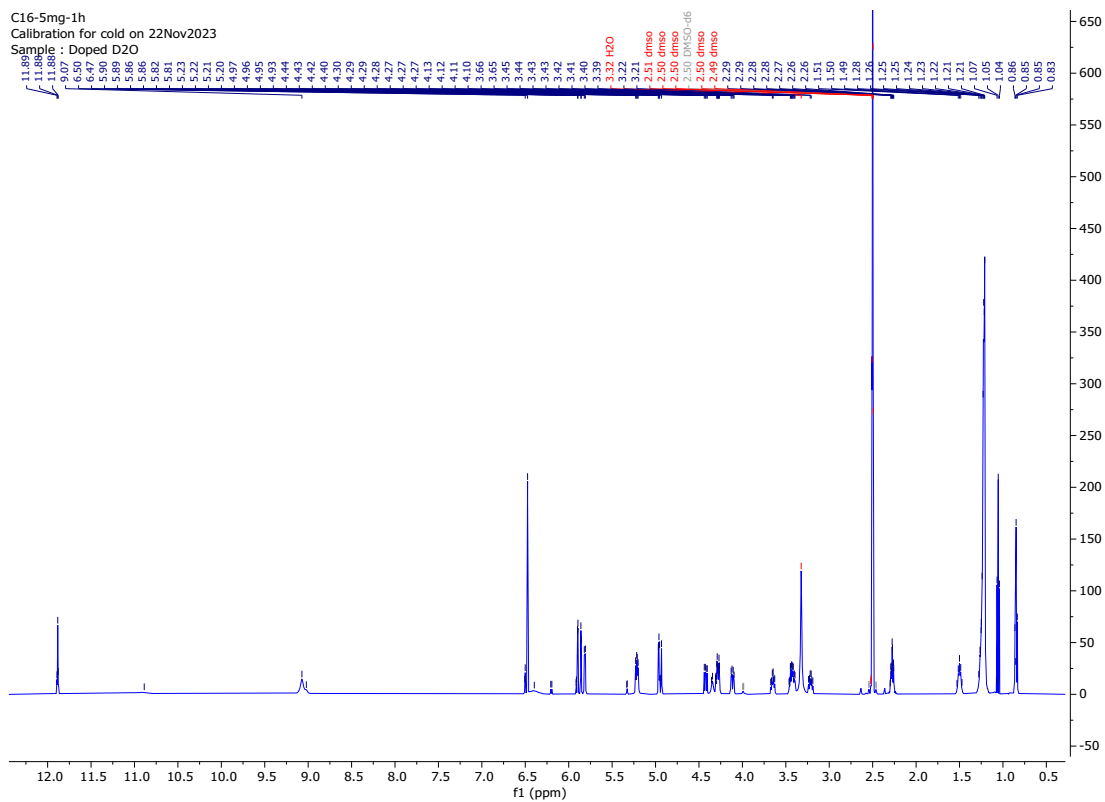


Figure S16. $^1\text{H-NMR}$ of dihydromyricetin 4'-O-(6-O-palmitoyl)- α -D-glucopyranoside (**2c**)

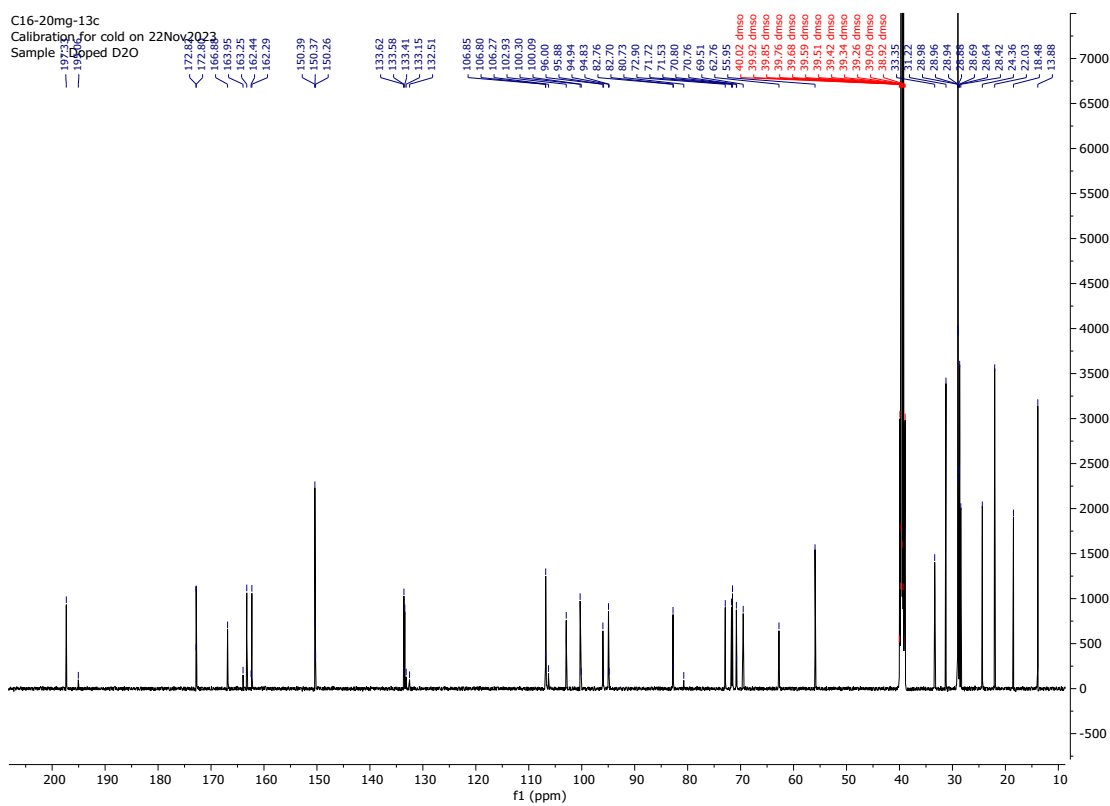


Figure S17. $^{13}\text{C-NMR}$ of dihydromyricetin 4'-O-(6-O-palmitoyl)- α -D-glucopyranoside (**2c**)

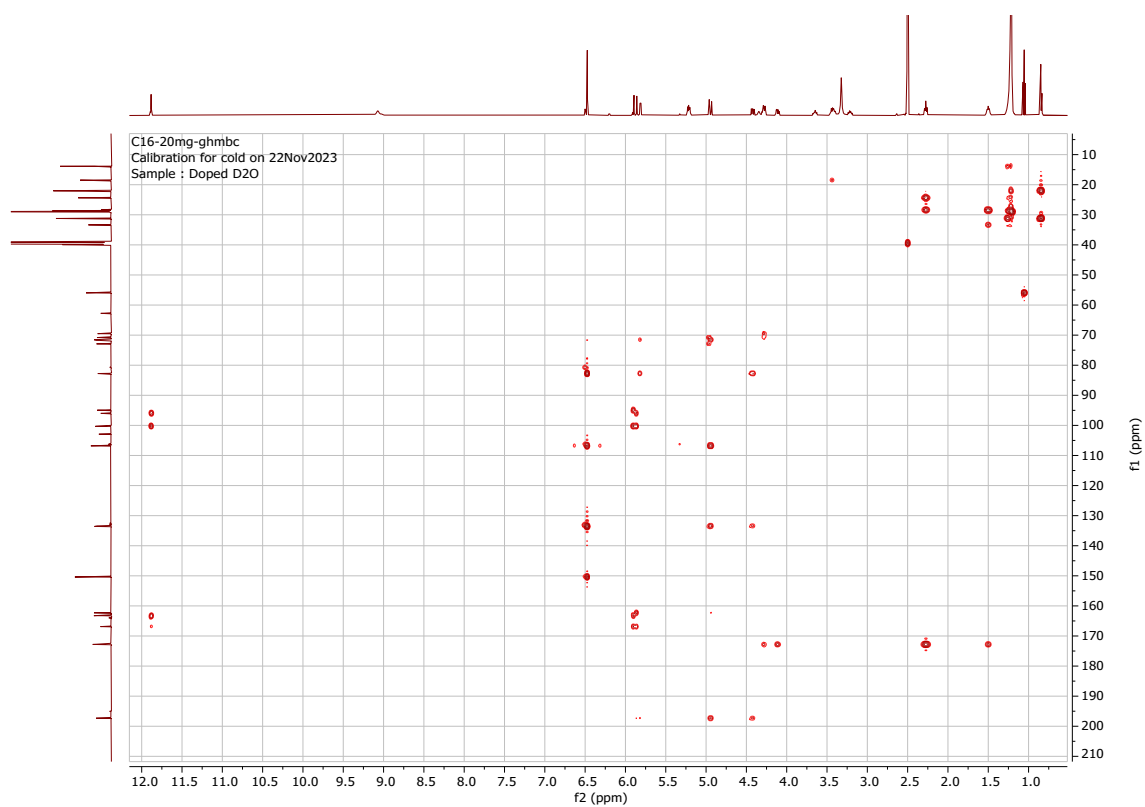


Figure S18. 2D-HMBC of dihydromyricetin 4'-O-(6-O-palmitoyl)- α -D-glucopyranoside (**2c**).